

JAAS

Accepted Manuscript



This is an *Accepted Manuscript*, which has been through the Royal Society of Chemistry peer review process and has been accepted for publication.

Accepted Manuscripts are published online shortly after acceptance, before technical editing, formatting and proof reading. Using this free service, authors can make their results available to the community, in citable form, before we publish the edited article. We will replace this *Accepted Manuscript* with the edited and formatted *Advance Article* as soon as it is available.

You can find more information about *Accepted Manuscripts* in the [Information for Authors](#).

Please note that technical editing may introduce minor changes to the text and/or graphics, which may alter content. The journal's standard [Terms & Conditions](#) and the [Ethical guidelines](#) still apply. In no event shall the Royal Society of Chemistry be held responsible for any errors or omissions in this *Accepted Manuscript* or any consequences arising from the use of any information it contains.

1
2
3 1
4
5
6 2 **Classification of the geographic origin of cigarettes according to Pb**
7
8
9 3 **isotope ratios by inductively coupled plasma dynamic reaction cell**
10
11
12 4 **mass spectrometry**
13
14
15
16 5

17
18 6 **Wei Guo ^a, Shenghong Hu ^{*, a}, Zhiwei Wu ^a, Gaoyong Lan ^a, Lanlan Jin ^a,**
19
20
21 7 **Xugui Pang ^b, Jincheng Zhan ^b, Bin Chen ^c, Zhiyong Tang ^d**
22
23
24 8

25
26 9 ^a *State Key Laboratory of Biogeology and Environmental Geology, China*
27
28
29 10 *University of Geosciences, Wuhan, 430074, P. R. China*
30

31
32 11 ^b *Shandong Geological Survey Institute, Jinan, 250013, P.R. China*
33

34
35 12 ^c *China National Environmental Monitoring Centre, Beijing, 100012, P.R. China*
36

37 13 ^d *Faculty of Materials Science and Chemistry, China University of Geosciences,*
38
39
40 14 *Wuhan, 430074, P. R. China*
41
42

43 15
44
45
46 16 **Corresponding Author**
47

48
49
50 17 *Tel. and Fax: +86-27-67883495. Email: shhu@cug.edu.cn
51
52
53 18
54
55
56
57
58
59
60

19 Abstract

20 Trace Pb is accumulated in the same isotopic ratio as it occurs in the source soil, and the isotopic
21 composition of Pb could be used to reflect these sources and provide powerful indicators of the
22 geographic origin of agricultural products. In this study, we developed a simple and valid method
23 based on inductively coupled plasma dynamic reaction cell mass spectrometry (ICP-DRC-MS)
24 for the determination of Pb isotope ratios to distinguish between the geographic origins of
25 cigarettes. The cigarette digestion solutions were directly analysed by ICP-DRC-MS with
26 pressuring a non-reactive gas Ne. In the DRC, Ne molecules collide with Pb ions and result in a
27 2.3-fold improvement in the average internal precision of Pb isotope ratios, which may be due to
28 the improvement of the ion transmission or sensitivity (via collisional focusing) and the
29 reduction of the plasma noise (via collisional energy damping). Under the optimum DRC
30 rejection parameter Q (RPq = 0.45), the main matrix components (K, Na, Ca, Mg, Al, Fe, *etc.*)
31 originating from cigarettes were filtered out. Other important parameters such as detector dead
32 time, dwell time per data acquisition and total integrated time per isotope were also optimized.
33 Mass discrimination of $^{208}\text{Pb}/^{206}\text{Pb}$ ratio in Ne DRC mode increased to 0.3% compared to the
34 vented mode, this mass bias could be accurately corrected by using the NIST 981 Pb isotope
35 standard solution. The accuracy and precision of this method were evaluated by using two
36 cigarette reference materials (Oriental tobacco leaves CTA-OTL-1 and Virginia tobacco leaves
37 CTA-VTL-2). Results of $^{208}\text{Pb}/^{206}\text{Pb}$ and $^{207}\text{Pb}/^{206}\text{Pb}$ were 2.0842 ± 0.0028 (2δ) and 0.8452
38 ± 0.0011 (2δ) for CTA-VTL-2, which were in agreement with the literature values ($^{208}\text{Pb}/^{206}\text{Pb} =$
39 2.0884 ± 0.0090 and $^{207}\text{Pb}/^{206}\text{Pb} = 0.8442 \pm 0.0032$), respectively. The Pb isotopic composition
40 ($^{208}\text{Pb}/^{206}\text{Pb} = 2.0812 \pm 0.0028$ and $^{207}\text{Pb}/^{206}\text{Pb} = 0.8460 \pm 0.0018$) of CTA-VTL-1 was reported for
41 the first time in our study. The precision of Pb isotope ratios ($^{208}\text{Pb}/^{206}\text{Pb}$ and $^{207}\text{Pb}/^{206}\text{Pb}$) for the

1
2
3 42 cigarette samples ranged from 0.05 to 0.12 % (N = 6). The proposed method has sufficient
4
5 43 precision to distinguish between 91 cigarette brands originated from four different geographic
6
7
8 44 regions.
9

10
11 45

16 46 **Introduction**

17
18
19 47 Although cigarette smoking kills approximately 6 million people worldwide and causes more
20
21 48 than 5000 billion dollars of economic damage each year ¹, the number of daily smokers increased
22
23 49 from 721 million in 1980 to 967 million in 2012 ². Cigarettes accounted for 80 %of the global
24
25
26 50 tobacco production of 5.2 million tons per year. The globalization of tobacco markets resulted in
27
28 51 easy tobacco trade between countries; however, the consumers are increasingly concerned about
29
30 52 the origin of their cigarettes. Therefore, rapid and valid profiling techniques should be
31
32
33 53 established to identify the geographic origin of cigarettes.
34
35

36 54 Plants accumulate trace metals from the soil and they are deposited on the foliage. Since the
37
38 55 elements are accumulated in the same isotopic ratios as they occur in the source soil, the isotopic
39
40 56 ratio reflects the sources and indicates the geographic origin of products derived from vegetative
41
42
43 57 matter³. The following two techniques based on isotopic ratio have been used to determine the
44
45
46 58 geographic origin of agricultural products: 1) isotope composition of light elements (H, B, C, N,
47
48 59 O, S, *etc.*) and 2) ratios of heavy elements (Sr, Pb, *etc.*) ⁴⁻¹¹. Compared to light elements, isotopes
49
50 60 of heavy elements are rarely fractionated in the terrestrial ecosystem, and the latter are more
51
52
53 61 advantageous for determining geographic origin ¹². In general, there is no difference in the
54
55
56 62 isotope ratio between a crop and its exchangeable fraction in the soil as long as the crop is grown
57
58 63 under the same soil and water conditions. Establishing the isotope ratio database of a product
59
60

1
2
3
4 64 helps to identify whether other new products belong to this category. The major fraction of Pb in
5
6 65 agricultural products originates from the soil and from secondary sources such as low amounts of
7
8 66 the substances, pesticides, fertilizers, vehicle exhaust, *etc.* The isotopic composition of Pb is of
9
10 67 particular interest because ^{208}Pb , ^{207}Pb and ^{206}Pb are derived from the radioactive decay of ^{232}Th ,
11
12 68 ^{235}U and ^{238}U , respectively ¹³. Large variations in Pb isotopic ratios (0.82–0.95 for $^{207}\text{Pb}/^{206}\text{Pb}$,
13
14
15 69 and 2.02–2.22 for $^{208}\text{Pb}/^{206}\text{Pb}$) are observed in environmental and soil samples because of the
16
17 70 differences in the formation and chemical composition of the rocks from which the ores were
18
19 71 formed ^{14,15}. Therefore, Pb isotope ratios inherit the geological character of a production area and
20
21 72 this factor has been used for determining the geographic origin of wine ¹⁵⁻¹⁷ and rice ¹⁸.

22
23
24
25 73 Although thermal ionization mass spectrometry (TIMS) and multi-collector inductively
26
27 74 coupled plasma mass spectrometry (MC-ICP-MS) are highly precise (<0.005%) and are
28
29 75 considered to be the best methods for measuring the Pb isotope ratios, they are very expensive
30
31 76 for regular use in most of the testing laboratories ¹⁹⁻²⁴. Quadrupole ICP-MS (ICP-QMS)
32
33 77 instruments are less expensive, higher sample throughput and are used in many laboratories.
34
35 78 However, this method is less poor precision (0.1–0.5%) compared to the TIMS and MC-ICP-MS
36
37 79 methods ²⁵⁻²⁹. Recently, Bandura *et al.* reported that collisional damping by a non-reactive gas
38
39 80 (Ar or Ne) in a dynamic reaction cell (DRC) results in improved precision of isotope ratios
40
41 81 (0.03~0.1%) ³⁰. It had been demonstrated that the collisions with the non-reactive gas molecules
42
43 82 increase the average residence time of the analyte ions in the cell and that ions sampled at
44
45 83 slightly different moments in time are actually mixed ³⁰. As a consequence, short-term
46
47 84 fluctuations of the ion signal intensities are damped and the precision of the isotope ratios are
48
49 85 improved ³⁰⁻³³. This method had been used for measuring the Pb isotope ratios in the atmosphere
50
51
52 86 ³¹, archaeological artefacts ³², snow and sediment ³⁴. However, the mass discrimination due to in-

1
2
3 87 cell fractionation effects also existed in these complex samples and a chromatographic extraction
4
5 88 step was required to separate Pb from the concomitant matrix ³¹⁻³³. Fortunately, the main
6
7
8 89 concomitant matrix (K, Na, Ca, Mg, Fe, Sr, Ba, *etc.*) of tobacco samples are less complex than
9
10 90 the soil or rock matrices; hence, mass discrimination due to matrix elements in the DRC may be
11
12 91 alleviated without subsequent isolation processes. The total Pb concentration of cigarettes in
13
14 92 various regions typically ranged from 0.5–6.5 $\mu\text{g/g}$ ³⁵⁻³⁸, which are sufficiently high
15
16
17 93 concentrations for measuring isotope ratios by ICP-QMS.

18
19
20 94 In this study, we present an analytical procedure for the determination of Pb isotope ratios in
21
22 95 cigarettes for classifying their geographic origin. We optimized the technique, its analytical
23
24 96 performance, as well as its application to the determination of Pb isotope ratios in 91 different
25
26 97 brands of cigarettes procured from seven countries. Differences in the Pb isotope ratios allowed
27
28 98 the evaluation of the proposed method as a potential tool for tracing cigarette provenance.
29
30
31
32 99

33 34 35 100 **Experimental**

36 37 38 39 101 **Instrumentation**

40
41
42
43 102 A PerkinElmer SCIEX ELAN DRC-e ICP-MS instrument was used. A PFA-400 MicroFlow
44
45 103 (self-absorption, 0.1 mL min^{-1}) nebulizer interfaced with a cyclonic spray chamber (PC³ Peltier
46
47 104 Chiller) was used with a 2.0 mm i.d quartz injector tube, which is described in detail elsewhere
48
49 105 ^{39,40}. The operating parameters of the DRC-ICP-MS are summarized in Table 1. Under the
50
51 106 optimized operating conditions, the sensitivity of ²⁰⁸Pb was $>15,000 \text{ cps/ng mL}^{-1}$. High purity Ar
52
53 107 and Ne gases (99.999% purity) for ICP-MS were purchased from Praxair Investment Co., Ltd,
54
55
56
57 108 China.
58
59
60

109 Reagents and standards

110 High purity water ($18.2 \text{ M}\Omega \text{ cm}^{-1}$) used for the preparation of all standards, blanks and sample
111 solutions was produced by a Millipore water purification system (Millipore, France). Nitric acid
112 (HNO_3 , 99.9999%), hydrofluoric acid (HF, 99.999%) and hydrogen peroxide (H_2O_2 , 99.999%)
113 were purchased from Alfa Aesar Ltd. (Tianjin). The Pb isotopic standard (1000 mg L^{-1}) was
114 prepared by dissolving 1 g of NIST SRM 981 in HNO_3 (Merck, Germany). Working standard
115 solutions were prepared daily by diluting the stock solution in 1% (v/v) HNO_3 . The accuracy and
116 precision of the method were evaluated by using two cigarette reference materials (RMs),
117 namely oriental tobacco leaves (CTA-OTL-1) and Virginia tobacco leaves (CTA-VTL-2),
118 obtained from the Institute of nuclear chemistry and technology (INCT), Warsaw, Poland. The
119 total Pb concentration of CTA-OTL-1 and CTA-VTL-2 were $4.88 \pm 0.14 \mu\text{g g}^{-1}$ and $22.1 \pm 0.4 \mu\text{g}$
120 g^{-1} , which were in good agreement with the certified values of $4.91 \pm 0.80 \mu\text{g g}^{-1}$ and 22.1 ± 1.2
121 $\mu\text{g g}^{-1}$, respectively.

122 Sampling and sample preparation

123 Seventy tobacco samples of various Chinese brands were purchased from 21 tobacco shops of
124 the China national tobacco corporation (CNTC). Other tobacco samples were purchased from the
125 overseas markets. Five brands (CAMEL-1, CAMEL-2, SHAMAN'S, MARLBORO-1 and
126 MARLBORO-2) were obtained from the United States, three brands (EXPORT, du MAURIER
127 and L&M) from Canada, three brands (TREASURER, KENT and LAMBERT & BUTLER)
128 from England, three brands (BLACK, ARDATH and BENTOEL) from Indonesia, two brands
129 (BACSON and AROMA) from Vietnam and five brands (TIME, ESSE LIGHTS, RAISON, ESSE
130 and TONINO LAMBORGHINI) from Korea. All the samples were stored in plastic bags and

1
2
3 131 refrigerated (4°C). The samples were oven-dried at 60°C and manually ground by using an agate
4
5 132 mortar to obtain the desired particle size ($\leq 75\mu\text{m}$). Following which, 250 mg of the powdered
6
7 133 sample was placed in a 25 mL home-made PTFE-lined stainless steel bomb. 3 mL of HNO_3 and
8
9 134 0.5 mL of HF were added to the bomb and heated at 120 °C to dryness (but not baked) on a hot
10
11 135 plate. After cooling, 3 mL of HNO_3 and 2 mL of H_2O_2 were added and the bomb was sealed and
12
13 136 placed in an electric oven and heated to 180 °C for 6 h. After cooling, the bomb was opened and
14
15 137 placed on a hot plate (at 120 °C), and evaporated to incipient dryness. Then, 1.0 mL of HNO_3
16
17 138 and 2.0 mL of ultra-pure water were added and the bomb was covered and gently heated to
18
19 139 extract Pb from the residues. The final solution was made up to 25 mL by adding ultra-pure
20
21 140 water. For the high Pb concentration ($22.1 \pm 1.2 \mu\text{g g}^{-1}$) of the CTA-VTL-2 RM, the dilution
22
23 141 factor was 1000-fold.
24
25
26
27
28
29
30
31

32 143 **Results and discussion**

33 34 35 36 144 **Collisional focusing for the precise measurement of Pb isotope ratios**

37
38
39 145 Application of ICP-QMS has been advantageous for measuring Pb isotope ratios because of the
40
41 146 high sample throughput, ease of sample preparation and low cost of analysis compared to other
42
43 147 techniques. However, poor precision ranging from 0.1–0.5% RSD ($^{208}\text{Pb}/^{206}\text{Pb}$ or $^{208}\text{Pb}/^{207}\text{Pb}$)
44
45 148 may be obtained with the traditional ICP-QMS (without reaction or collision cell)^{41,42}, thus
46
47 149 making it difficult to distinguish between the Pb sources from different geographical origins;
48
49 150 therefore, efforts should be made to improve precision. In this study, Ne, a non-reactive gas, was
50
51 151 studied as a DRC collision gas for improving the precision of Pb isotope ratios. Fig. 1a shows the
52
53 152 effect of increasing Ne flow on the average internal precision (ratio RSD of 5 replicates was
54
55
56
57
58
59
60

1
2
3
4 153 measured 6 times and then the average of 6 RSDs taken) of $^{208}\text{Pb}/^{207}\text{Pb}$ for 10 ng mL^{-1} of the
5
6 154 NIST 981 standard solution. As shown in Fig. 1a, the advantage in terms of precision is
7
8 155 significant, the precision improved 2.3-fold by the pressurized DRC mode ($\text{Ne} = 0.3 \text{ mL min}^{-1}$)
9
10 156 compared to the DRC vented mode ($\text{Ne} = 0$), which is similar to the values (~ 2.5 fold) reported
11
12 157 by Bandura *et al.*³⁰ and Resano *et al.*⁴¹ The ratio RSD (average internal precision) for the
13
14 158 pressurized cell ($\text{Ne} = 0.3 \text{ mL min}^{-1}$) is 0.072% with a corresponding counting statistics error (SE)
15
16 159 of 0.069%, whereas for the vented mode ($\text{Ne} = 0$) it is 0.17% and 2.5 times higher than the
17
18 160 counting SE (Fig. 1a). Fig. 1b shows the effects of the average internal precision and the
19
20 161 counting SE as a function of the total counts of ^{208}Pb and ^{206}Pb , the average internal precision
21
22 162 follows closely the counting SE at the selected range. On the other hand, the signal intensities of
23
24 163 ^{208}Pb and ^{206}Pb were enhanced by up to 3 times with pressurized cell ($\text{Ne} = 0.3 \text{ mL min}^{-1}$), which
25
26 164 is due to the improvement of the ion transmission (via collisional focusing) (Fig. 1c). A high
27
28 165 counts could be beneficial for obtaining the high precision isotope ratios, but the sensitivity
29
30 166 improvement could only improve 1.7-fold (square root of 3) for the precision, as a result, there
31
32 167 may be other factors affect the precision. Bandura *et al.*³⁰ demonstrated that short-term ion signal
33
34 168 fluctuations are damped by the collisions with a high Ne gas flow ($1.5\text{-}2.0 \text{ mL min}^{-1}$), and the
35
36 169 precision of isotope ratios are improved. To avoid large mass discrimination (Fig. 4) and
37
38 170 collisional scattering, a low Ne gas flow (0.30 mL min^{-1}) was selected in our study. Therefore,
39
40 171 we speculate that the ion transmission or sensitivity improved by collisional focusing, in
41
42 172 combination with the reducing plasma noise by collisional energy damping, results in a better
43
44 173 precision. Another important parameter is the rejection parameter Q (RPq) of DRC. In this study,
45
46 174 the optimum RPq value of 0.45 (Table 1) provided the best transmission efficiency in the DRC
47
48 175 when operated in the pressurized mode. Meanwhile, an RPq value of 0.45 for an m/z of 206
49
50
51
52
53
54
55
56
57
58
59
60

1
2
3 176 results in a cut-off at approximately $m/z = 102$ ⁴¹, resulting in the filtering out of the main matrix
4
5 177 components (K, Na, Ca, Mg, Al, Fe, *etc.*) of the cigarettes. Therefore, a combination of high
6
7
8 178 sensitivity, low matrix effect and improved plasma noise with collisional damping result in an
9
10
11 179 improved precision of Pb isotope ratios.

14 180 **Optimization of the data acquisition parameters**

17 181 Data acquisition parameters such as detector dead time, dwell time per data acquisition and total
18
19
20 182 measurement time per isotope should be optimized to obtain best precision while measuring
21
22 183 isotope ratios by ICP-QMS. The dead time associated with detector response leads to counting
23
24 184 losses that increase in magnitude with increasing counting rate⁴³. This leads to inconsistencies in
25
26
27 185 the isotope abundance ratio measurements that are independent of mass discrimination effects;
28
29 186 therefore, the inconsistencies must be corrected prior to correcting mass discrimination. The
30
31
32 187 detector dead time was determined according to a method proposed by Nelm *et al.*⁴⁴. The results
33
34 188 of the ²⁰⁶Pb/²⁰⁸Pb isotope ratio measurements versus dead time applied in the software are
35
36 189 presented in the ICP-DRC-MS data shown in Fig. 2. Dead time was determined from the dead
37
38
39 190 times corresponding to each intersection point and a value of 53 ns was obtained from
40
41 191 calculations (Fig. 2). The obtained value was in agreement with the manufacturer's
42
43
44 192 recommended value (55 ns for DRC-e ICP-MS) and it was similar to the reported values (61 ns
45
46 193 for DRC *plus* ICP-MS)⁴¹. As shown in Fig. 3a, the best precision (0.03–0.05% for ²⁰⁸Pb/²⁰⁶Pb and
47
48 194 ²⁰⁸Pb/²⁰⁷Pb) was obtained at dwell time values of 1, 2 and 2ms for ²⁰⁸Pb, ²⁰⁶Pb and ²⁰⁷Pb,
49
50
51 195 respectively. The optimum total measurement time per replicate was also evaluated by changing
52
53 196 the number of sweeps and/or readings from 1 to 1000. When the value was higher than 59 s per
54
55
56 197 replicate measurement, no improvement in precision was observed as shown in Fig. 3b. In

1
2
3 198 addition, the optimum replicate was selected as five times because precision remained constant
4
5 199 from 5 to 11 times of replication. The total measurement time was 5 min 46 s per sample. Other
6
7
8 200 optimized parameters are listed in Table 1.
9

10 11 201 **Mass bias correction and analytical performance**

12
13
14
15 202 Mass discrimination effects should also be corrected for accurate isotope ratio determination.
16
17 203 Mass discrimination is the bias between the experimental value (after correcting detector dead
18
19
20 204 time and procedure blank) and the corresponding ‘true’ value. Some studies^{45,46} reported that the
21
22 205 collision gas in the collision/reaction cell affects mass discrimination. Xie *et al.*⁴⁵ reported that
23
24 206 for a quadrupole-based instrument equipped with a radio frequency (rf) only hexapole collision
25
26
27 207 cell, the use of He and H₂ does not affect mass discrimination. However, Boulyga and Becker
28
29 208 reported that the use of He resulted in the collisional focusing of heavier ions, while the lighter
30
31
32 209 ions suffered from collisional scattering, leading to mass discrimination.⁴⁶ Therefore, it is
33
34 210 important to investigate the mass discrimination of Ne in DRC for the determination of Pb
35
36 211 isotope ratios in tobacco samples. In our preliminary experiments, a digested solution (20 ng mL⁻¹
37
38 212 ¹) of CTA-VTL-2 was used to study the effect of Ne gas flow rate on the ²⁰⁸Pb/²⁰⁶Pb isotope
39
40 213 ratios. As shown in Fig. 4, Pb isotope ratios increased with increasing Ne flow rate. At the
41
42
43 214 optimum Ne gas flow rate of 0.3 mL min⁻¹, the ²⁰⁸Pb/²⁰⁶Pb ratio increased by 0.3% (from 2.0848
44
45 215 to 2.0911) compared to the standard mode (DRC vented). Mass bias due to the in-cell Ne gas
46
47
48 216 collision can be accurately corrected because both the cigarette samples and isotopic standards
49
50 217 are measured under the same conditions. The measurement sequence consisted of 1% HNO₃
51
52 218 blank, 20 ng mL⁻¹ NIST SRM 981 Pb standard solution, produce blank, sample 1, NIST 981
53
54 219 standard, sample 2, NIST 981 standard and so on. The obtained Pb isotope ratios were corrected
55
56
57
58
59
60

for mass discrimination by the external bracketing technique and the true sample ratios ($R_{\text{true, sample}}$) were calculated as follow:

$$R_{\text{true, sample}} = R_{\text{NIST, cert}} * \frac{R_{\text{detect, sample}}}{\frac{R_{\text{NIST, before}} + R_{\text{NIST, after}}}{2}}$$

where $R_{\text{NIST, cert}}$ is the certified value of NIST SRM 981 common Pb given by NIST. $R_{\text{detect, sample}}$ is the value after the blank correction procedure. After the above correction, the Pb isotope ratio was 2.0848 ± 0.0028 for $^{208}\text{Pb}/^{206}\text{Pb}$, which is consistent with that of the vented mode (2.0849 ± 0.0063). Two cigarettes RMs (CTA-OTL-1 and CTA-VTL-2) were used to evaluate the accuracy of the proposed method and their Pb isotope ratios are summarized in Table 2. For the CTA-VTL-2 RMs, $^{208}\text{Pb}/^{206}\text{Pb}$ and $^{207}\text{Pb}/^{206}\text{Pb}$ were 2.0848 ± 0.0028 and $0.8452 \pm 0.0011(2\delta)$, respectively. Reproducibility ranged from 0.046–0.076% ($N = 27$) for the CTV-VTL-2 RM (Fig. 5) and a little upward trend of $^{208}\text{Pb}/^{206}\text{Pb}$ did not influence precision. Since the Pb isotope ratio values were not certified in both the RMs, the accuracy of the Pb isotope ratio measurements in the tobacco RMs were assessed by literature values. The detected values were in agreement with the values reported by Judd *et al.*³⁵, but the precision obtained in this study was obviously better than the reported values (Table 2). Pb isotopic composition is not yet published for the CTA-OTL-1 RM, for which our detected values were $^{208}\text{Pb}/^{206}\text{Pb} = 2.0812 \pm 0.0028$ and $^{208}\text{Pb}/^{206}\text{Pb} = 0.8460 \pm 0.0018 (2\delta)$ (Table 2). To confirm the value, ten separate aliquots of CTA-OTL-1 were digested and analysed in a period of three months. These analyses yielded Pb isotope ratio values ranging from 2.0809–2.0814 (average of 2.0812 ± 0.0029) for $^{208}\text{Pb}/^{206}\text{Pb}$ and 0.8457 to 0.8463 (average of 0.8461 ± 0.0016) for $^{208}\text{Pb}/^{206}\text{Pb}$, respectively. These values are in agreement with the above values (Table 2).

Classification of the geographic origin of cigarettes

1
2
3 241 A total of 91 brands of cigarette samples from seven different countries were analysed by using
4
5 242 the proposed method. When the dilution factor was fixed at 100-fold, the total Pb concentrations
6
7 243 ranged from 7–49 ng mL⁻¹. Since the accuracy and precision values of Pb isotope ratios did not
8
9 244 vary at Pb concentrations ranging from 5–80 ng mL⁻¹ (Fig. 6), the digested solutions of the
10
11 245 cigarette samples were directly measured by this method. Various brands fall into four distinct
12
13 246 categories based on the ²⁰⁸Pb/²⁰⁶Pb and ²⁰⁷Pb/²⁰⁶Pb ratios as shown graphically in Fig. 7. Each
14
15 247 point represents one sample and the error bars are twice the standard deviation of each
16
17 248 measurement (2δ). The average internal precision (N = 6) of Pb isotope ratios (²⁰⁸Pb/²⁰⁶Pb and
18
19 249 ²⁰⁷Pb/²⁰⁶Pb) ranged from 0.05–0.12% for the cigarette samples. The ²⁰⁸Pb/²⁰⁶Pb and ²⁰⁷Pb/²⁰⁶Pb
20
21 250 ratios are statistically different at the *p* = 0.05 level or better between each group: the ²⁰⁸Pb/²⁰⁶Pb
22
23 251 values of three cigarette brands originated from England (2.1295–2.1378) are higher than that of
24
25 252 the other groups (2.0528–2.1180), and the ²⁰⁷Pb/²⁰⁶Pb values of cigarettes originated from
26
27 253 Indonesia (0.8621–0.8656) are higher than that of the other three groups (0.8366–0.8580). The
28
29 254 ²⁰⁸Pb/²⁰⁶Pb and ²⁰⁷Pb/²⁰⁶Pb ratios of the cigarettes originated from North America (0.8353–
30
31 255 0.8431 and 2.0528–2.0818) are lower than that of the other three groups (0.8456–0.8656 and
32
33 256 2.0813–2.1180). The Pb isotope ratios of cigarettes originated from East Asia (China, Korea and
34
35 257 Vietnam) fall within the middle of the plot (Fig. 7). Interestingly, the ²⁰⁸Pb/²⁰⁶Pb ratio of one
36
37 258 Chinese brand (Liquan) was high at 2.22 as reported by Judd *et al.*³⁵; however, the ²⁰⁸Pb/²⁰⁶Pb
38
39 259 ratios of cigarettes from 70 Chinese brands ranged from 2.08–2.13 (Fig. 7). This difference
40
41 260 (>5%) is far beyond the measured precision. To explain this phenomenon, 16 Liquan cigarette
42
43 261 samples (five kinds) collected from eight tobacco shops of CNTC were measured and the
44
45 262 ²⁰⁸Pb/²⁰⁶Pb ratios ranged between 2.09 and 2.11 (Table S1 of the ESI.[†]), which fall within the
46
47 263 range of 2.08–2.13. The difference of ²⁰⁸Pb/²⁰⁶Pb ratios occurred may be due to the only one
48
49
50
51
52
53
54
55
56
57
58
59
60

1
2
3 264 Liqun brand sample was analysed in Judd's paper ³⁵, and was collected from the general store
4
5
6 265 (not collected from the manufacturer of CNTC). Since the cigarettes originated from China,
7
8 266 Korea and Vietnam have similar Pb isotope ratios, these different cigarette brands cannot be
9
10 267 discriminated, which as well as the cigarettes from USA and Canada.
11
12
13
14 268
15
16

17 269 **Conclusions**

20 270 The proposed technique is simple, valid and has sufficient precision to distinguish between the
21
22 271 different cigarettes brands originated from four different geographic regions. Further research is
23
24 272 necessary to measure large number of cigarette samples produced from different regions and to
25
26 273 generate a complete geographic database of Pb isotope ratios for classifying the geographic
27
28 274 origin and to distinguish counterfeit cigarettes from legal samples.
29
30
31
32
33
34 275
35

36 276 **Acknowledgments**

37
38
39 277 This work was supported by the National Nature Science Foundation of China (No. 21207120,
40
41 278 21175120), the National Key Scientific Instrument and Equipment Development Projects of
42
43 279 China (No. 2011YQ06010008), and the Fundamental Research Funds for the Central
44
45 280 Universities, China University of Geosciences (Wuhan) (No. CUGL140411).
46
47
48
49
50 281
51
52

53 282 **References**

54
55
56
57
58
59
60

- 1
2
3 283 1. World Health Organization. WHO report on the global tobacco epidemic.
4
5 284 http://www.who.int/tobacco/global_report/2013/summary/en/. 2013.
6
7
8 285 2. M. Ng, M. K. Freeman, T.D. Fleming, M. Robinson, T. B. Dwyer-Lindgren, A. Wollum, E.
9
10 286 Sanman, S. Wulf, A. D. Lopez, C. J. L. Murray, and E. Gakidou E, *JAMA*, 2014, **311**, 183-
11
12 287 192.
13
14
15 288 3. D. M. A. M. Luykx, and S. M. Van Ruth, *Food Chem.*, 2008, **107**, 897-911.
16
17
18 289 4. G. Francois, L. Gaillard, M-H, Salagoity, and B. Medina, *Anal. Bioanal. Chem.*, 2011, **401**,
19
20 290 1551-1558.
21
22 291 5. S. Branch, S. Burke, P. Evans, B. Fairman, and C. S. J. W. Briche, *J. Anal. At. Spectrom.*,
23
24 292 2003, **18**, 17-22.
25
26
27 293 6. M. Barbaste, K. Robinson, S. Guifoyle, B. Medina, and R. Lobinski, *J. Anal. At. Spectrom.*,
28
29 294 2002, **17**, 135-137.
30
31
32 295 7. F. C. L. Bontempo, K. Heinrich, M. Horacek, S. D. K. C. Schlicht, F. Thomas, F. J. Monahan,
33
34 296 J. Hoogewerff, and A. Rossmann, *Anal. Bioanal. Chem.*, 2007, **389**, 309-320.
35
36
37 297 8. G. Fortunato, K. Mumic, S. Wunderli, L. Pillonel, J. O. Bosset, and G. Gremaud, *J. Anal. At.*
38
39 298 *Spectrom.*, 2004, **19**, 227-234.
40
41
42 299 9. H. Forstel, *Anal. Bioanal. Chem.*, 2007, **388**, 541-544.
43
44 300 10. S. Husted, B. F. Mikkelsen, J. Jensen, and N. E. Nielsen, *Anal. Bioanal. Chem.*, 2004, **378**,
45
46 301 171-182.
47
48
49 302 11. P. P. Coetzee, and F. Vanhaecke, *Anal. Bioanal. Chem.*, 2005, **383**, 977-984.
50
51 303 12. K. Arivama, M. Shinozaki, and A. Kawasaki, *J. Agric. Food Chem.*, 2012, **60**, 1628-1634.
52
53 304 13. A. Dicken, Radiogenic Isotope Geology, Cambridge University Pree, Cambridge, 1995.
54
55 305 14. J. Barling, and D. Weis, *J. Anal. At. Spectrom.*, 2012, **27**, 653-662.
56
57
58
59
60

- 1
2
3 306 15. X. D. Tian, H. Emteborg, M. Barbaste, and F. C. Adams, *J. Anal. At. Spectrom.*, 2000, **15**,
4
5 307 829-835.
6
7
8 308 16. C. M. R. Almeida, and M. T. S. D. Vasconcelos, *J. Agri. Food Chem.*, 2003, **51**, 3012-3023.
9
10 309 17. K. Arivama, M. Shinozaki, and A. Kawasaki, *J. Agric. Food Chem.*, 2012, **60**, 1628-1634.
11
12 310 18. M. Barbaste, L. Halicz, A. Galy, B. Medina, H. Emteborg, F. C. Adams, and R. Lobinski,
13
14 311 *Talanta*, 2011, **54**, 307-317.
15
16 312 19. I. Smet, D. De Muynck, F. Vanhaecke, and M. Elburg, *J. Anal. At. Spectrom.*, 2010, **25**,
17
18 313 1025-1032.
19
20 314 20. V. N. Epov, D. Malinovskiy, F. Vanhaecke, D. Begue, and O. F. X. Donard, *J. Anal. At.*
21
22 315 *Spectrom.*, 2011, **26**, 1142-1156.
23
24 316 21. L. Font, G. van der Peijl, L. van Wetten, P. Vroon, B. van der Wagt, and G. Davies, *J. Anal.*
25
26 317 *At. Spectrom.*, 2012, **27**, 719-732.
27
28 318 22. G. S. Ortega, C. Pecheyran, S. Berail, and O. F. X. Donard, *J. Anal. At. Spectrom.*, 2012, **27**,
29
30 319 1447-1456.
31
32 320 23. F. Vanhaecke, L. Balcaen, and D. Malinovsky, *J. Anal. At. Spectrom.*, 2009, **24**, 863-886.
33
34 321 24. R. N. Taylor, O. Ishizuka, A. Michalik, J. A. Milton, and I. W. Croudace, *J. Anal. At.*
35
36 322 *Spectrom.*, **2014**, DOI: 10.1039/C4JA00279B.
37
38 323 25. Y. C. Yip, J. C. W. Lam, and W. F. Tong, *TRAC-Trend. Anal. Chem.*, 2008, **27**, 460-480.
39
40 324 26. J. Vogl, B. Paz, M. Koenig, and W. Pritzkow, *Anal. Bioanal. Chem.*, 2013, **405**, 2995-3000.
41
42 325 27. M. Dronov, and J. Schram, *J. Anal. At. Spectrom.*, 2013, **28**, 1796-1803.
43
44 326 28. C. Standish, B. Dhuime, R. Chapman, C. Coath, C. Hawkesworth, and A. Pike, *J. Anal. At.*
45
46 327 *Spectrom.*, 2013, **28**, 217-225.
47
48 328 29. A. Bazzano, and M. Crotti, *J. Anal. At. Spectrom.*, 2014, **29**, 926-933.
49
50
51
52
53
54
55
56
57
58
59
60

- 1
2
3 329 30. D. R. Bandura, V. I. Baranov, and S. D. Tanner, *J. Anal. At. Spectrom.*, 2000, **15**, 921-928.
4
5
6 330 31. B. P. Jackson, P. V. Winger, and P. J. Lasier, *Environ. Pollut.* 2004, **130**, 445-451.
7
8 331 32. D. De Muynck, C. Cloquet, and F. Vanhaecke, *J. Anal. At. Spectrom.*, 2008, **23**, 62-71.
9
10 332 33. F. Vanhaecke, L. Balcaen, I. Deconinck, I. D. Schrijver, C. M. Almeida, and L. Moens, *J.*
11
12 *Anal. At. Spectrom.*, 2003, **18**, 1060-1065.
13
14 334 34. A. Bazzano, and M. Grotti, *J. Anal. At. Spectrom.*, 2014, **29**, 926-933.
15
16 335 35. C. D. Judd, and K. Swami, *Isot. Environ. Healt. S.*, 2010, **46**, 484-494.
17
18 336 36. R. J. O'Connor, Q. Li, W. E. Stephens, D. Gammond, T. Elton-Marshall, K. M. Cummings,
19
20 G. A. Giovino, and G. T. Fong, *Tab. Control.*, 2011, **19 (S2)**, i47-i53.
21
22 337
23 338 37. S. G. Musharraf, M. Shoaib, A. J. Siddiqui, M. Najam-ul-Haq, and A. Ahmed, *Chem. Cent.*
24
25 *J.*, 2012, **6**, 56-67.
26
27 339
28 340 38. S. Verma, S. Yadav, and I. Singh, *Food Chem. Toxicol.*, 2010, **48**, 2291-2297.
29
30 341 39. W. Guo, S. H. Hu, J. Y. Zhang, L. L. Jin, X. J. Wang, Z. L. Zhu, and H. F. Zhang, *J. Anal.*
31
32 *At. Spectrom.*, 2011, **26**, 2076-2080.
33
34 342
35 343 40. W. Guo, S. H. Hu, X. J. Wang, J. Y. Zhang, L. L. Jin, Z. L. Zhu, and H. F. Zhang, *J. Anal.*
36
37 *At. Spectrom.*, 2011, **26**, 1198-1230.
38
39 344
40 345 41. M. Resano, P. Marzo, J. Perez-Arantequi, M. Aramendia, C. Cloquet, and F. Vanhaecke, *J.*
41
42 *Anal. At. Spectrom.*, 2008, **23**, 1182-1191.
43
44 346
45 347 42. S. D. Tanner, V. I. Baranov, and D. R. Bandura, *Spectrochim. Acta Part B*, 2002, **57**, 1361-
46
47 1452.
48
49 348
50 349 43. K. E. Jarvis, A. L. Gray, and R. S. Houk, Handbook of inductively coupled plasma mass
51
52 spectrometry. Blackie, Glasgow, 1992, ch.11, p312.
53
54
55
56
57
58
59
60

- 1
2
3 351 44. S. M. Nelm, C. R. Quetel, T. Prohaska, J. Vogl, and P. D. P. Taylor, *J. Anal. At. Spectrom.*,
4
5 352 2011, **26**, 333-338.
6
7
8 353 45. Q. L. Xie, and R. Kerrich, *J. Anal. At. Spectrom.*, 2002, **17**, 69-74.
9
10 354 46. S. F. Boulyga, and J. S. Becker, *J. Anal. At. Spectrom.*, 2002, **17**, 965-966.
11
12
13 355
14
15
16
17
18
19
20
21
22
23
24
25
26
27
28
29
30
31
32
33
34
35
36
37
38
39
40
41
42
43
44
45
46
47
48
49
50
51
52
53
54
55
56
57
58
59
60

1
2
3
4 356 **Figure captions**
5
6

7 357 **Fig.1** (a) Average RSD (%) for the $^{208}\text{Pb}/^{206}\text{Pb}$ and $^{207}\text{Pb}/^{206}\text{Pb}$ ratios ($N = 6$, replicate = 5) as a
8
9 358 function of the Ne collision gas flow rate, dotted lines show counting statistics error SE; (b)
10
11 359 $^{208}\text{Pb}/^{206}\text{Pb}$ average internal precision for the pressurized with Ne at 0.3 mL min^{-1} cell and its
12
13 360 corresponding counting SE as a function of the total accumulated counts; (c) Pb signal intensities
14
15 361 as a function of the Ne collision gas flow rate.
16
17
18

19
20 362 **Fig.2** $^{206}\text{Pb}/^{208}\text{Pb}$ ratio *versus* dead time.
21
22

23 363 **Fig.3** Optimization of the dwell time per acquisition point (a) and the total measurement time per
24
25 364 replicate (b) for Pb isotopic ratios in 20 ng mL^{-1} NIST SRM 981 Pb solution by ICP-DRC-MS
26
27 365 with 0.3 mL min^{-1} Ne as the collision gas.
28
29
30

31 366 **Fig.4** Effects of the Ne collision gas flow rate in DRC on the $^{208}\text{Pb}/^{206}\text{Pb}$ ratios in a digested
32
33 367 solution (20 ng mL^{-1}) of the CTA-VTL-2 Virginia Tobacco Leaves.
34
35
36

37 368 **Fig.5** Results of repeated analyses of a 20 ng mL^{-1} tobacco SRM CTA-VTL-2 solution. Average
38
39 369 values of the NIST 981 corrected Pb isotope ratios are: $^{208}\text{Pb}/^{206}\text{Pb} = 2.0842 \pm 0.0009$ and
40
41 370 $^{207}\text{Pb}/^{206}\text{Pb} = 0.8452 \pm 0.0015$ (2δ). The measured time is twenty-seven ($N = 27$).
42
43
44

45 371 **Fig.6** Effects of the total Pb concentrations in the analyzed solution on the values of the accuracy
46
47 372 and precision Pb ratios. Pb concentrations were ranged from 5 to 80 ng mL^{-1} of the NIST SRM
48
49 373 981 Pb solution.
50
51
52

53 374 **Fig.7** Results for lead isotope ratios in 91 different brands of cigarette originated from seven
54
55 375 different countries, plot of $^{208}\text{Pb}/^{206}\text{Pb}$ against $^{207}\text{Pb}/^{206}\text{Pb}$.
56
57
58
59
60

376 **Tables**377 **Table 1** Instrument operating parameters

ICP-MS instrument	Perkin-Elmer Sciex Elan DRC-e
Sample introduction	PFA-400 MicroFlow nebulizer (self sample absorption)
Spray chamber	Cyclonic spray chamber (PC ³ Peltier Chiller)
Injector tube	2.0 mm id Quartz
Interface cones	Ni, 1.1 mm i.d. for sampling cone, and 0.9 mm i.d. for skimmer cone.
RF power, W	1100
Plasma gas flow, L min ⁻¹	15
Auxiliary gas flow, L min ⁻¹	1.00
Nebulizer gas flow, L min ⁻¹	0.85
Lens Voltage, V	8.0
Autolens	Off
DRC parameters	
Cell gas Ne, mL min ⁻¹	0.30
Rejection parameter, q	0.45
Rejection parameter, a	0
QRO	-6
CRO	-1
CPV	-15
Data acquisition parameters	
Scanning mode	Peak hopping
Detector mode	Pulse counting
Detector dead time	53 ns
Dwell time	2 ms for ²⁰⁶ Pb ⁺ and ²⁰⁷ Pb ⁺ , 1 ms for ²⁰⁸ Pb ⁺

Settling time	200 μ s
Sweeps	600
Readings	20
Replicate	5
Total measurement time	5 min 46 s per sample

378

1
2
3
4
5
6
7
8
9
10
11
12
13
14
15
16
17
18
19
20
21
22
23
24
25
26
27
28
29
30
31
32
33
34
35
36
37
38
39
40
41
42
43
44
45
46
47
48
49
50
51
52
53
54
55
56
57
58
59
60

379

380 **Table 2** Pb isotope ratios of the two tobacco standard reference materials (CTA-VTL-2 and
 381 CTA-OTL-1) by this method

	This work		Reference ratios (2 δ), Judd et al. (2010)	
	Measured ratios (2 δ)	Average internal precision (N =5), % ^a		
CTA-VTL-2	²⁰⁸ Pb/ ²⁰⁶ Pb	2.0842±0.0028	0.051	2.0884±0.0090
	²⁰⁷ Pb/ ²⁰⁶ Pb	0.8452±0.0011	0.072	0.8442±0.0032
CTA-OTL-1	²⁰⁸ Pb/ ²⁰⁶ Pb	2.0812±0.0028	0.049	/ ^b
	²⁰⁷ Pb/ ²⁰⁶ Pb	0.8460±0.0018	0.068	/

382 ^a Ratio RSD of 5 replicates was measured 6 times, then the average of 7 RSDs taken

383 ^b Non certified and literature reported value

384

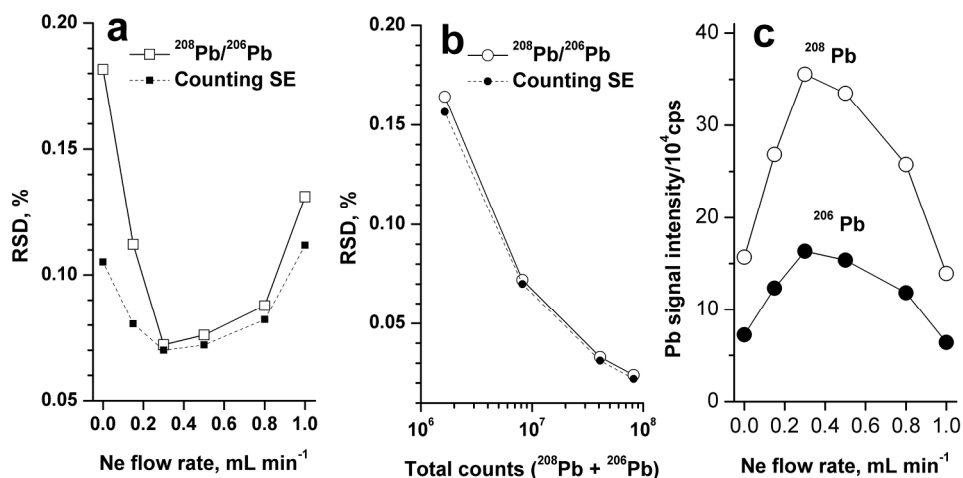


Fig.1 (a) Average RSD (%) for the $^{208}\text{Pb}/^{206}\text{Pb}$ and $^{207}\text{Pb}/^{206}\text{Pb}$ ratios (N = 6, replicate = 5) as a function of the Ne collision gas flow rate, dotted lines show counting statistics error SE; (b) $^{208}\text{Pb}/^{206}\text{Pb}$ average internal precision for the pressurized with Ne at 0.3 mL min⁻¹ cell and its corresponding counting SE as a function of the total accumulated counts; (c) Pb signal intensities as a function of the Ne collision gas flow rate.
210x148mm (300 x 300 DPI)

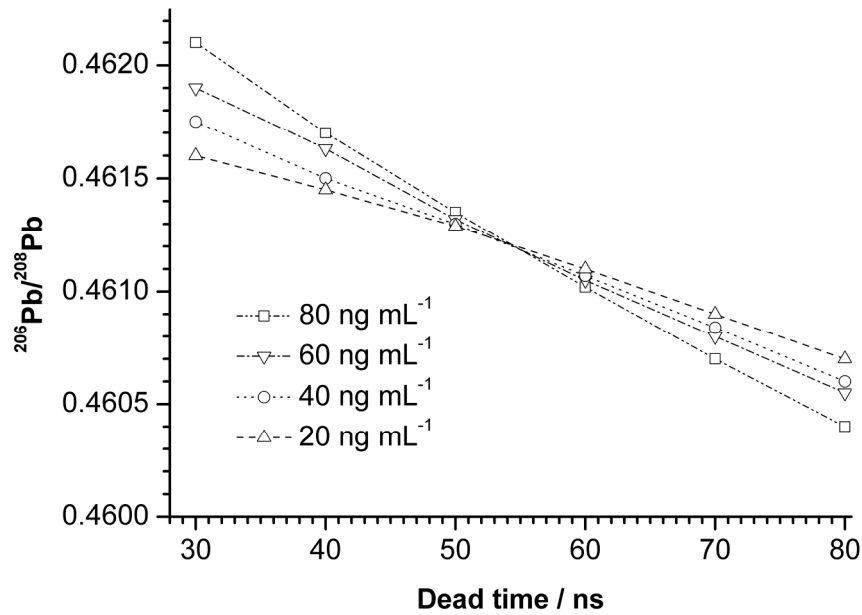


Fig.2 $^{206}\text{Pb}/^{208}\text{Pb}$ ratio versus dead time.
210x148mm (300 x 300 DPI)

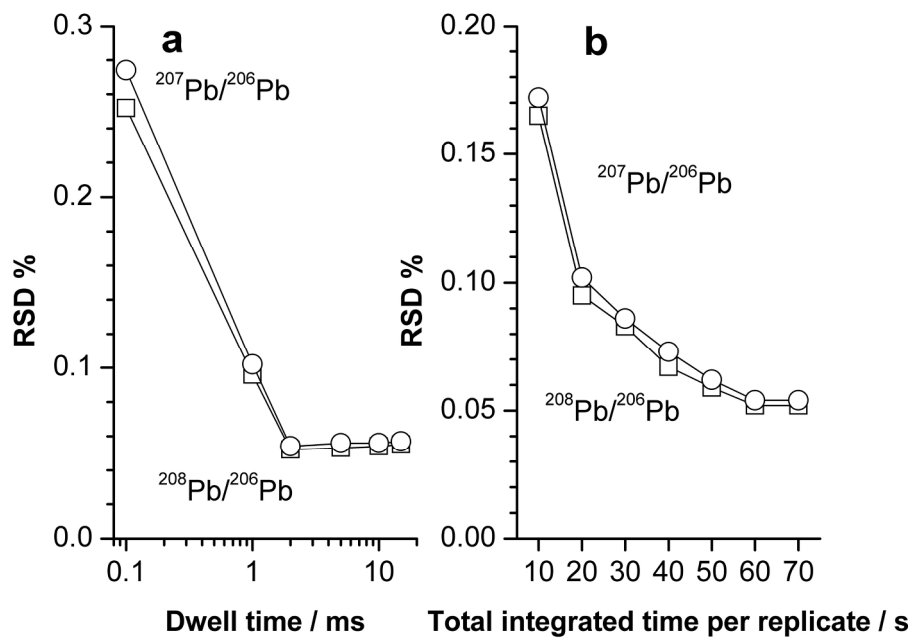


Fig.3 Optimization of the dwell time per acquisition point (a) and the total measurement time per replicate (b) for Pb isotopic ratios in 20 ng mL^{-1} NIST SRM 981 Pb solution by ICP-DRC-MS with 0.3 mL min^{-1} Ne as the collision gas.
210x148mm (300 x 300 DPI)

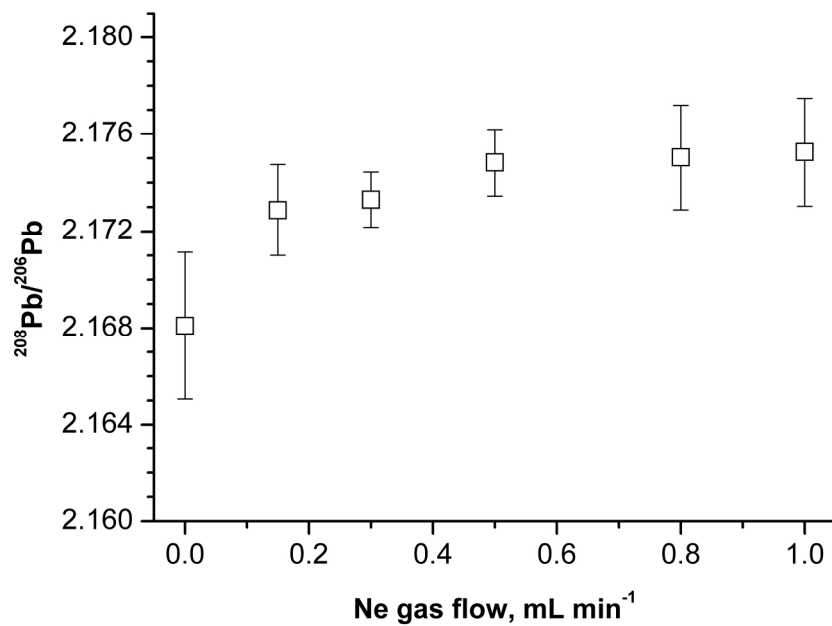


Fig.4 Effects of the Ne collision gas flow rate in DRC on the $^{208}\text{Pb}/^{206}\text{Pb}$ ratios in a digested solution (20 ng mL⁻¹) of the CTA-VTL-2 Virginia Tobacco Leaves.
210x148mm (300 x 300 DPI)

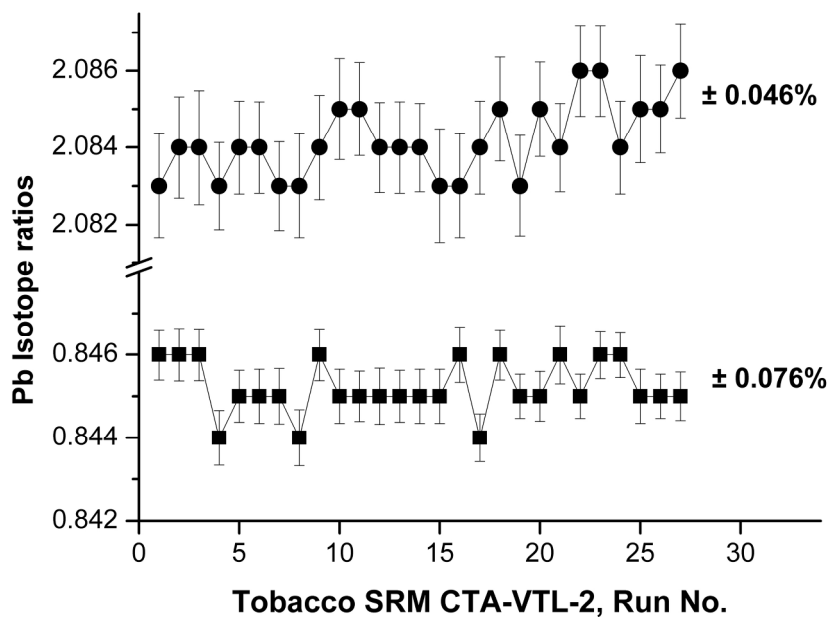


Fig.5 Results of repeated analyses of a 20 ng mL^{-1} tobacco SRM CTA-VTL-2 solution. Average values of the NIST 981 corrected Pb isotope ratios are: $^{208}\text{Pb}/^{206}\text{Pb} = 2.0842 \pm 0.0009$ and $^{207}\text{Pb}/^{206}\text{Pb} = 0.8452 \pm 0.0015$ (2δ). The measured time is twenty-seven ($N = 27$).
210x148mm (300 x 300 DPI)

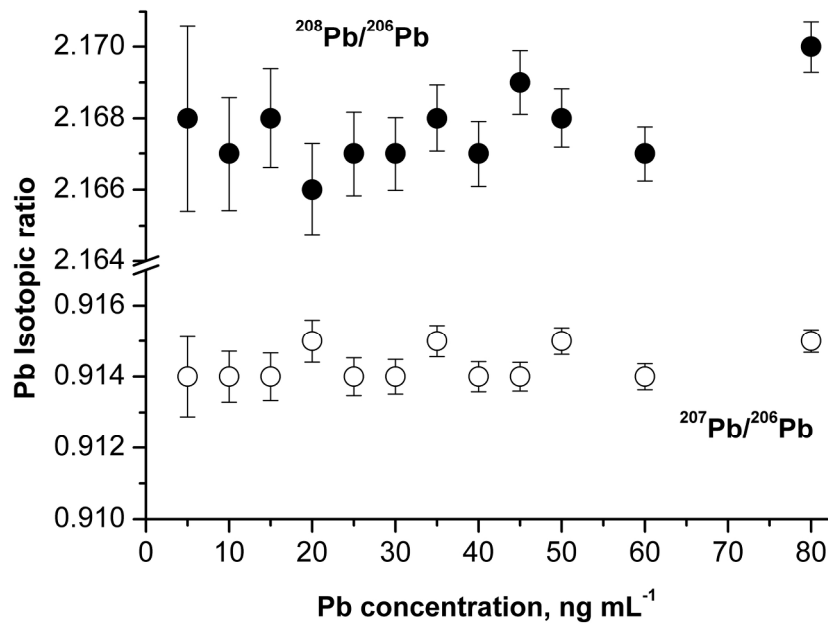


Fig.6 Effects of the total Pb concentrations in the analyzed solution on the values of the accuracy and precision Pb ratios. Pb concentrations were ranged from 5 to 80 ng mL^{-1} of the NIST SRM 981 Pb solution. 210x148mm (300 x 300 DPI)

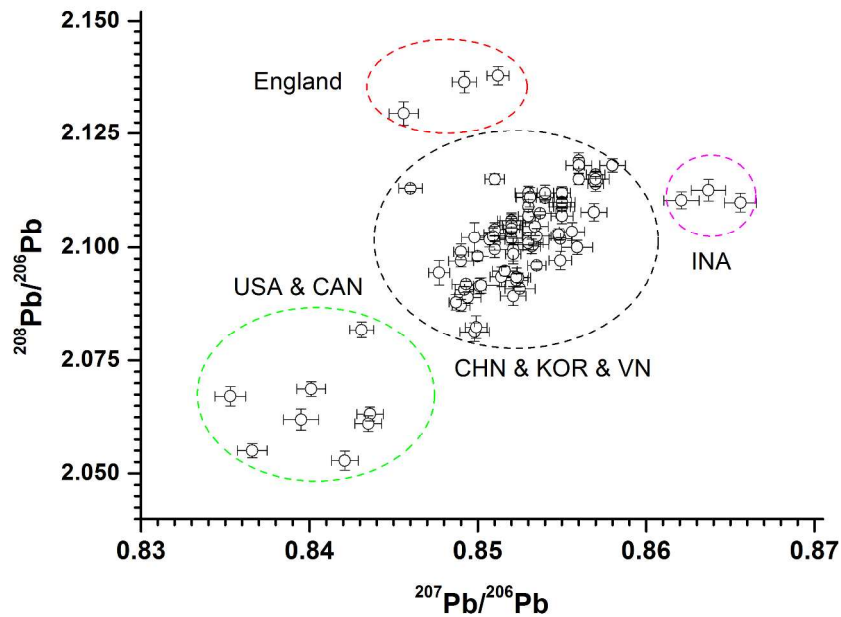


Figure 7 Results for lead isotope ratios in 91 different brands of cigarette originated from seven different countries, plot of $^{208}\text{Pb}/^{206}\text{Pb}$ against $^{207}\text{Pb}/^{206}\text{Pb}$.
297x210mm (300 x 300 DPI)